OR4-6

軌道上微小重力環境におけるろ紙の燃え拡がり

Flame Spread over Filter Papers in orbital microgravity environments

小林芳成 [1], 高橋周平 [1], 鳥飼宏之 [2], 菊池政雄 [3], 藤田修 [4]
Yoshinari KOBAYASHI[1], Shuhei TAKAHASHI[1], Hiroyuki TORIKAI[2], Masao KIKUCHI[3] and Osamu FUJITA[4]
[1] 岐阜大学，Gifu University
[2] 弘前大学，Hirosaki University
[3] 宇宙航空研究開発機構，Japan Aerospace Exploration Agency
[4] 北海道大学，Hokkaido University

1. Introduction

To develop spacecraft fire safety technologies available for future space explorations, Prof. Fujita (Hokkaido Univ., Japan) proposed research entitled "Fundamental Research on International Standard of Fire Safety in Space—base for safety of future manned mission—." That proposal was accepted in 2012 by the Japan Aerospace Exploration Agency (JAXA) as a research project for the third-phase utilization of the Japanese experiment module "Kibo" on the International Space Station (ISS). This project is named "FLARE" (Flammability Limits At Reduced-g Experiment) and still ongoing as of August, 2023. The FLARE project is internationally organized by 14 institutes from 4 countries including JAXA, NASA, ESA, CNES, and DLR. These institutes are divided into four research groups, three of which will perform on-orbit experiments in the Kibo on the ISS. On May 19th, 2022, the first space experiment on the flame spread over filter paper sheets has been successfully completed. This paper then presents the experimental results of the flame spread experiments on the ISS/Kibo and discusses the flame spread characteristics of the filter paper sheets—the limiting oxygen concentration (LOC), flame spread rate, length of the preheat zone, etc.— The findings from this work would deepen our understanding of the flame spread over solid fuels in low-flow velocity region, which much contributes to the development of spacecraft fire safety techniques and standards.

2. Experiment

The flame spread experiments of the filter paper sheets were performed by the Solid Combustion Experiment Module (SCEM) aboard the ISS, which was developed by the JAXA and IHI inspection & Instrumentation Co. and launched to the ISS on May 21st, 2020, illustrated in Fig. 1a. The SCEM had a combustion vessel with a volume of L220 × H375 × W550 mm where an experimental apparatus called "Experiment Insert," shown in Fig. 1b, was loaded. As shown in Fig. 1c, the experiment insert had a circulation fan and honeycombs for rectification to produce a uniform circulating flow. The forced flow could be accelerated up to 25 cm/s and varied stepwise during the experiments. Pressure and oxygen concentration inside the combustion vessel could be elevated up to 101.3 kPa and 45% by controlling a volume balance between nitrogen and oxygen gases. Pressure, oxygen concentration, and temperature were constantly monitored during the experiments by pressure sensors, an oxygen sensor, and thermocouples. Note that oxygen concentration would decrease by ~1% when a filter paper sheet was completely burned. A sample card with a filter paper sheet was automatically suppled to a test section by a sample feeder. That card was also automatically sent to a recovery cartridge after the flame spread experiment was completed. The filter paper sheets were ignited by a 0.4-mm-thick kanthal wire coil, and then a flame did spread along or against the flow parallel to the sheets. Two ignitors were located upstream and downstream respectively, and therefore both concurrent- and opposed-flow flame spread were achieved. Five cameras—three digital cameras (SVS-VISTEK, evo8051CFLGEA), a high-speed camera (IDT, Os10-4K), and an infrared camera (Vision Sensing, VIM-640G2U)—were set around the combustion vessel to record the flame spread behaviors from the top and side. Tested filter paper sheets (Advantec No. 4A) were 130 mm long, 40 mm wide, and 0.12 mm thick. According to the type of sample cards shown in Fig. 1d, the width of burned part was decreased to be 20 mm.

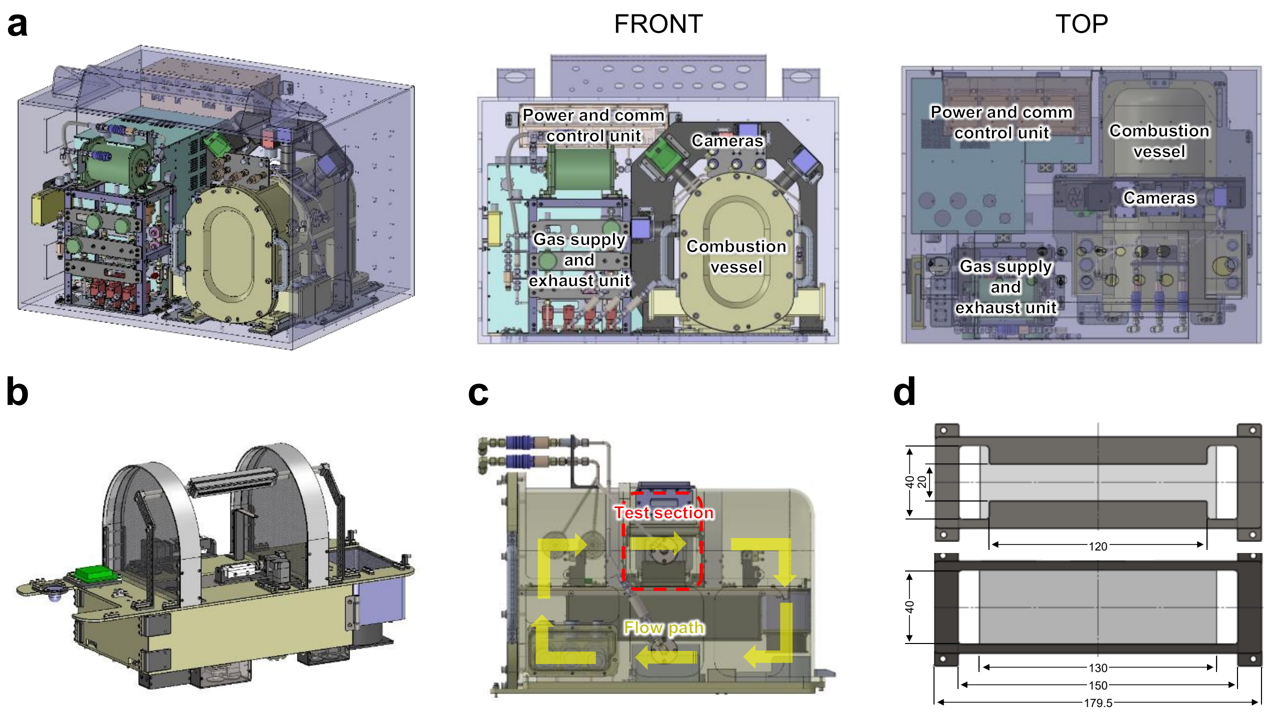

Figure 1. Schematic of (a) Solid Combustion Experiment Module (SCEM), (b) Experiment Insert 2, (c) test section and flow path in the SCEM, and (d) the two types of sample cards.

3. Results and discussion

3.1. Flame spread behaviors

In oxygen concentrations higher than the estimated LOCs, a two-dimensional planar flame was developed to steadily spread, which is often observed on the ground. Even in lower oxygen concentrations, however, a flame could spread at quite a low rate. This was very surprising to the authors because they initially expected that the flame could not survive under the estimated LOCs, in particular at an opposed-flow velocity of 0 cm/s. In fact, however, the flame changed its shape to a tiny, curved flame like "flamelet" and did spread in a zigzag manner even in such extreme environments. If the "flamelet spread" is considered as "flame spread," then the flame-spread limit would extend toward low opposed-flow velocity. Figure 2 is a group of snapshots that show a representative flame spread behavior of the two types of flame spread. For the 2D flame spread in Fig. 2a, a flame was developed to fill the sample width of 20 mm and did spread relatively fast, as seen from its position per 10 s. For the flamelet spread in Fig. 2b, on the other hand, a flame was tiny and did spread not straight but in zigzag. Such flame spread behaviors are similar to fingering behaviors in smoldering combustion. For the filter papers, flaming combustion usually occurs, but non-flaming combustion, i.e., smoldering or glowing combustion, is found to happen in narrow channels or microgravity environments[1-5]. Such environments suppress the supply of oxidizer to the flame to develop the fingering instability. Consequently, the increased fingering instability produces many different fingering patterns. Although the spread behaviors in Fig. 2b involve the small flame, they would be much concerned with the fingering behaviors in smoldering combustion. In fact, the flamelet spread often appeared neat the LOC or in low-velocity conditions. The flame spread rate for the flamelet spread was much lower than that for the 2D flame spread rate, which is also similar to the characteristics of the fingering behaviors.

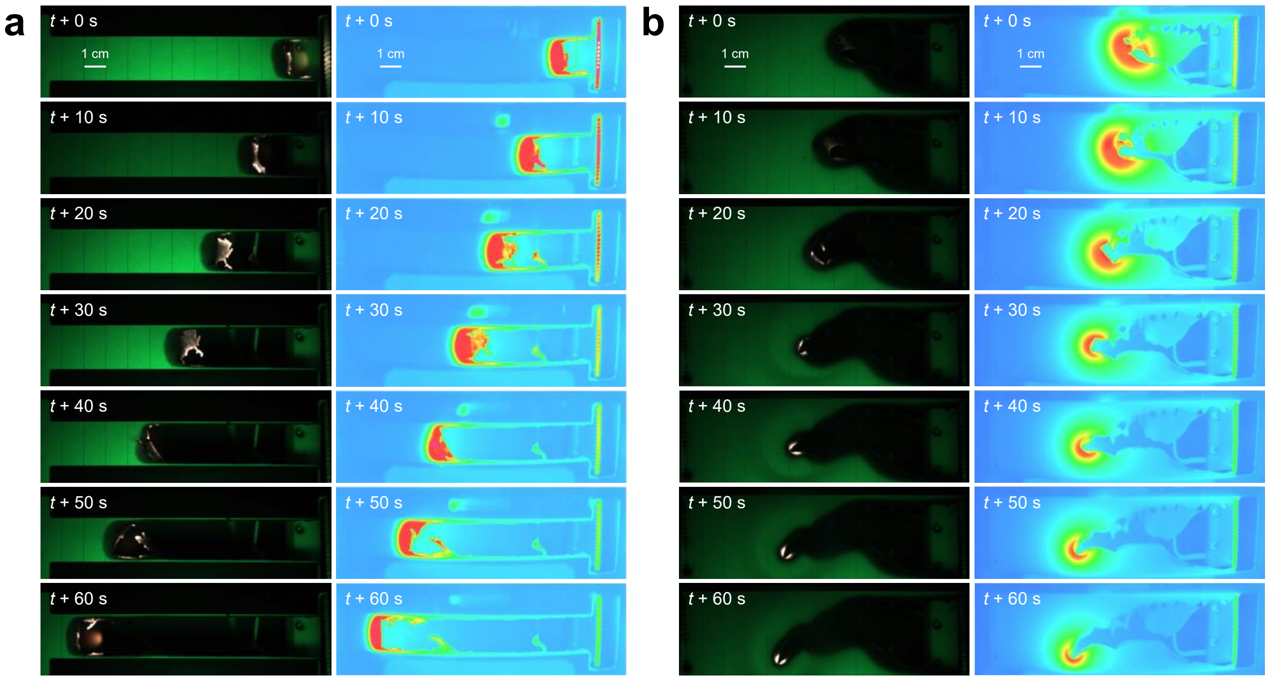

Figure 2. Snapshots of (a) 2D flame spread at an opposed-flow velocity of 20 cm/s in an oxygen concentration of 17.5% and (b) flamelet spread at an opposed-flow velocity of 0 cm/s in an oxygen concentration of 21.1%.

3.2. Flame spread rates

Figure 3a plots the flame spread rates over the flammability map of the filter paper sheets, and Fig. 3b represents the flame spread rates in different oxygen concentrations as a function of opposed-flow velocity. The flame spread rates for the 2D flame spread were mostly higher than 1 mm/s. In addition, at opposed-flow velocity of more than 10 cm/s, the flame spread rates were distributed in a narrow range between 1.0 mm/s and 1.5 mm/s and almost constant regardless of the opposed-flow velocity. Fundamentally, the opposed-flow flame spread is categorized into the three regimes: the radiative (or microgravity), thermal, and kinetic regimes[6,19,20]. Among those three regimes, both the radiative and chemical kinetic effects are not much significant in the thermal regime. When these two effects are not considered, a conclusion that the flame spread rate is independent from the opposed-flow velocity is yield. From the result in Fig. 3, therefore, the opposed-flow velocity range of at least 10–25 cm/s would be under the thermal regime. If the opposed-flow velocity is further increased, the flame spread rate would start decreasing at a certain velocity. This is because a transition would occur from the thermal regime to the kinetic regime where the finite-rate kinetics in the gas phase is important. At high opposed-flow velocities, the residence time approaches the chemical time, and eventually the flame would not be able to spread constantly when these two characteristic times become comparable. For the flamelet spread, on the other hand, the flame spread rates were mainly lower than 1 mm/s. Similar spread rates were reported by the past study where the flame spread over filter papers in a narrow channel and microgravity environment[2,5].

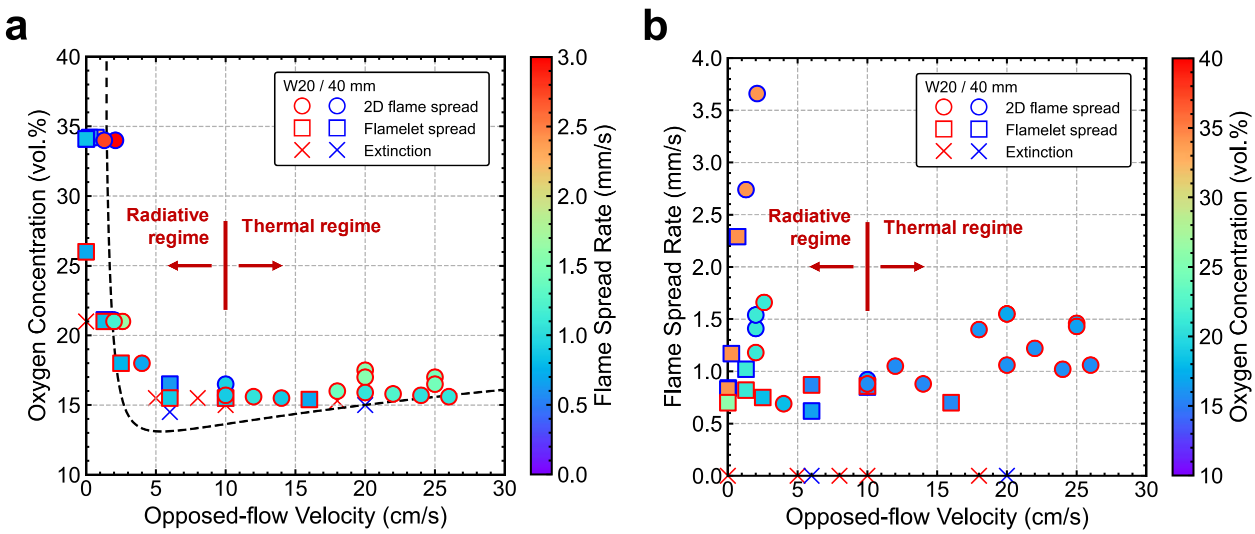

Figure 3. (a) Flame spread rates plotted over the flammability map and (b) those in different oxygen concentrations as a function of opposed-flow velocity.

3.3. Preheating length

As the flame spread rate in the last section, this work also calculated the length of preheat zone, i.e., the preheating length, to quantify and discuss the preheat zone. The preheating length was defined as the distance from the flame leading edge to the front of the preheat zone at a temperature of ~300℃. The preheating lengths were plotted over the flammability map of the filter paper sheets in Fig. 4a and as a function of opposed-flow velocity in Fig. 4b. The preheating length decreased with increased opposed-flow velocity. According to a scaling theory[6-8], the preheating length is inversely proportional to the opposed-flow velocity, and therefore a small/large preheat zone is produced at a high/low flow velocity. Such analytical trend was found to be experimentally correct from Fig. 4. Figure 2 also shows that the flamelet spread with no opposed-flows had a much longer preheating length than that for the 2D flame spread at an opposed-flow velocity of 20 cm/s. At less than 10 cm/s, in particular 2–3 cm/s, assumed to be the radiative regime, the preheating length was as long as 5–7 mm. The re-radiative heat transfer rate from the surface to the surroundings depends on the size of the preheat zone, and thus the re-radiative heat loss becomes significant with the preheating length. In the radiative regime where the preheating length was long, therefore, the increased re-radiative heat loss would reduce the net heat transfer rate for the flame spread to decrease the flame spread rate. When the net heat transfer rate falls below the heat transfer rate necessary for driving the flame spread, the flame would be extinct, that is, the radiative extinction would occur. On the other hand, in the thermal regime where the 2D flame spread was often observed, the preheating length ranged between about 3–5 mm and the dependence of the opposed-flow velocity was not much found.

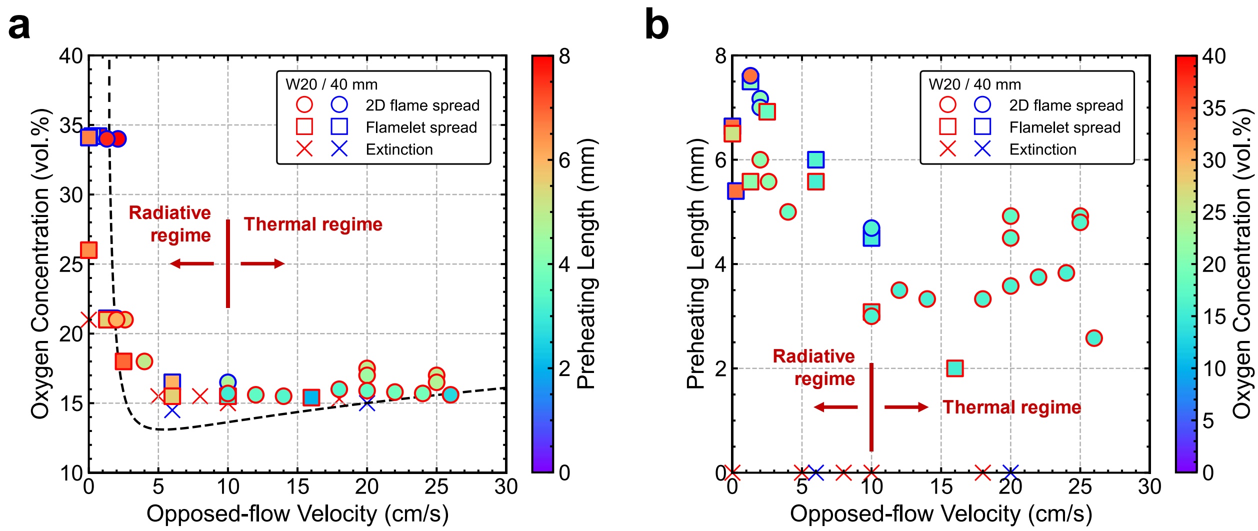

Figure 4. (a) Preheating lengths plotted over the flammability map and (b) those in different oxygen concentrations as a function of opposed-flow velocity.

4. Conclusions

This work performed the opposed-flow flame spread tests for the filter paper sheets by the SCEM aboard the ISS as the first campaign of the FLARE project, which was the first solid combustion experiment in the JEM "Kibo." The filter paper sheets were combusted in microgravity environments of variable oxygen concentration and opposed-flow velocity, and those flame spread behaviors were observed by the digital and IR cameras. At first, the authors anticipated that the extinction would happen in oxygen concentrations less than the LOCs. Particularly in quiescent environments, the extinction was expected to always occur no matter how high oxygen concentrations was. Contrary to that expectation, however, the flame survived by transforming its shape from the two-dimensional planar flame to the tiny, curved flame such as "flamelet." The flamelet did spread not straight but in zigzag at quite low rates. Such three-dimensional flame spread, i.e., the flamelet spread, was often observed in the radiative regime. The 2D flame spread, on the other hand, frequently appeared in the thermal regime. The flame spread rate and the preheating length for the flamelet spread were much lower and longer than those for the 2D flame spread. If the flamelet spread is considered another mode of the flame spread, then the flame-spread limit would be more extended. These data and findings from this work would help to validate the methodology to quantitatively predict the flame-spread limit and would deepen our understanding of the physics of the flame spread over solid fuels in the combustion science.

Acknowledgments

The authors acknowledge the support of the JAXA Human Spaceflight Technology Directorate for the sponsorship of the FLARE project.

References

1) Y. Zhang, P.D. Ronney, E.V. Roegner, J.B. Greenberg: Lewis number effects on flame spreading over thin solid fuels, Combust. Flame., **90** (1992) 71, DOI: 10.1016/0010-2180(92)90136-D.
2) S.L. Olson, H.R. Baum, T. Kashiwagi: Finger-like smoldering over thin cellulosic sheets in microgravity, Symp. (Int.) Combust., **27** (1998) 2525, DOI: 10.1016/S0082-0784(98)80104-5.
3) O. Zik, E. Moses: Fingering instability in solid fuel combustion: The characteristic scales of the developed state, Symp. (Int.) Combust., **27** (1998) 2815, DOI: 10.1016/S0082-0784(98)80139-2.
4) O. Zik, E. Moses: Fingering instability in combustion: An extended view, Phys. Rev. E., **60** (1999) 518, DOI: 10.1103/PhysRevE.60.518.
5) S.L. Olson, F.J. Miller, S. Jahangirian, I.S. Wichman: Flame spread over thin fuels in actual and simulated microgravity conditions, Combust. Flame., **156** (2009) 1214, DOI: 10.1016/j.combustflame.2009.01.015.
6) S. Takahashi, M. Kondou, K. Wakai, S. Bhattacharjee: Effect of radiation loss on flame spread over a thin PMMA sheet in microgravity, Proc. Combust. Inst., **29** (2002) 2579, DOI: 10.1016/S1540-7489(02)80314-5.
7) S. Bhattacharjee, K. Wakai, S. Takahashi: Predictions of a critical fuel thickness for flame extinction in a quiescent microgravity environment, Combust. Flame., **132** (2003) 523, DOI: 10.1016/S0010-2180(02)00501-1.
8) S. Bhattacharjee, S. Takahashi, K. Wakai, C.P. Paolini: Correlating flame geometry in opposed-flow flame spread over thin fuels, Proc. Combust. Inst., **33** (2011) 2465, DOI: 10.1016/j.proci.2010.06.053.